PHOTON–PHOTON SCATTERING IN THE RESONANCE REGION AT MIDRAPIDITY AT THE LHC*

Rainer Schicker[a], Mariola Kłusek-Gawenda[b]
Antoni Szczurek[b,c]

[a]Physikalisches Institut, Universität Heidelberg, Germany
[b]Institute of Nuclear Physics Polish Academy of Sciences, 31-342 Kraków, Poland
[c]Faculty of Mathematics and Natural Sciences, University of Rzeszów, Poland

(Received March 7, 2019)

A study is presented to extend the measurements of photon–photon scattering in ultra-peripheral Pb–Pb collisions at the LHC into the mass region of the pseudoscalar resonances η and η'. The elementary photon–photon scattering cross section is presented. The cross section for photon–photon scattering in Pb–Pb is derived by convoluting the elementary photon–photon cross section with the Pb–Pb photon luminosity. The main background to two-photon final states, arising from double π^0 production with two of the four decay photons escaping detection, is examined, and possible kinematical conditions are discussed to optimize the signal-to-background ratio for such measurements at mid-rapidity.

DOI:10.5506/APhysPolBSupp.12.793

1. Introduction

Classical electrodynamics is epitomised by Maxwell's equations

$$\partial_\alpha F^{\alpha\beta} = \frac{4\pi}{c} J^\beta\,, \qquad \partial_\alpha \mathcal{F}^{\alpha\beta} = 0\,. \tag{1}$$

The Maxwell equations in vacuum are linear in the electromagnetic fields $\boldsymbol{E}$ and $\boldsymbol{B}$. Two electromagnetic waves will pass through each other without scattering. The superposition principle conveniently expresses the non-interaction of electromagnetic fields at the classical level. The electromagnetic field energy carried by the electron, however, poses a conceptual challenge at the classical level. Attempts to circumvent the infinite Coulomb energy of a point charge resulted in the Born–Infeld electrodynamics which affirms the linearity of Maxwell's equations down to some length scale intrinsic to the electron, and introduces non-linear equations for smaller lengths

* Presented at the Diffraction and Low-x 2018 Workshop, August 26–September 1, 2018, Reggio Calabria, Italy.

scales [1]. The polarisation of the vacuum in view of Dirac's positron theory led to the Euler–Kockel–Heisenberg Lagrangian which modifies the classical Maxwell's equation in vacuum by leading non-linear terms [2]. The advent of accelerating heavy-ions at the LHC has opened up the possibility of measuring the photon–photon scattering cross section due to the large associated photon luminosity of the heavy-ion beams. Evidence of such events have been reported by the ATLAS and CMS collaborations at the LHC [3, 4]. These measurements are, however, restricted to photon–photon invariant masses $W_{\gamma\gamma} > 5$ and 6 GeV for the CMS and ATLAS data, respectively. The purpose of the analysis presented here is to study the feasibility of measuring photon–photon scattering in the range OF $0.4 < W_{\gamma\gamma} < 5$ GeV. As a first step, we analyse the corresponding cross section in this range, and examine the background which is dominated by π^0 pair production with only two of the four decay photons being within the detector acceptance.

2. The elementary photon–photon scattering cross section

Different mechanisms contribute to the elementary $\gamma\gamma \to \gamma\gamma$ scattering.

In Fig. 1, the different mechanisms of $\gamma\gamma$ scattering are presented. On the left, the loop diagram for fermions, leptons and quarks, is shown. In the centre, a QCD correction is displayed corresponding to a three-loop mechanism. On the right, the analogous process as expressed in the vector dominance approach is shown [5].

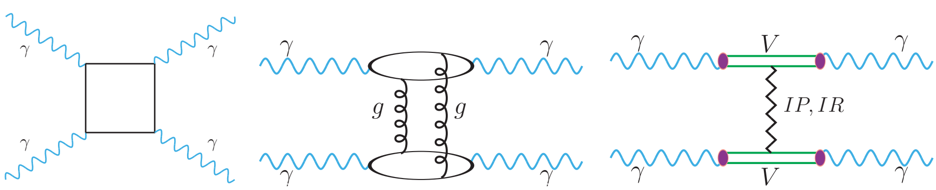

Fig. 1. Mechanisms of $\gamma\gamma \to \gamma\gamma$ scattering (figure taken from Ref. [5]).

3. Photon–photon scattering in ultra-peripheral heavy-ion reactions

The cross section for photon–photon scattering in ultra-peripheral heavy-ion collisions can be calculated by folding the cross section of the elementary mechanisms shown in Fig. 1 with the equivalent photon flux [6],

$$N(\omega, b) = \frac{Z^2\alpha}{\pi^2}\frac{1}{\beta^2 b^2}\left|\int_0^\infty \mathrm{d}v\, v^2 J_1(v)\frac{F_{\mathrm{el}}\left(-\frac{u^2+v^2}{b^2}\right)}{u^2+v^2}\right|^2 . \tag{2}$$

Here, ω denotes the energy of the photon, and b represents the transverse distance from the centre of the nucleus where the photon density is evaluated. The integral in Eq. (2) represents the form factor of the charge distribution of the source.

The cross section for $\gamma\gamma \to \gamma\gamma$ in PbPb collisions is calculated by convoluting the elementary cross section with the photon flux of Eq. (2)

$$\sigma^{\mathrm{EPA}}_{\mathrm{PbPb}\to\mathrm{PbPb}\gamma\gamma} = \int\!\!\int \mathrm{d}n^1_\gamma \, \mathrm{d}n^2_\gamma \, \sigma_{\gamma\gamma\to\gamma\gamma}(\omega_1, \omega_2) \, . \tag{3}$$

The differential cross section for photon–photon scattering in PbPb collisions at $\sqrt{s} = 5.02$ TeV resulting from the convolution of Eq. (3) is shown in Fig. 2. This cross section is derived with the box diagrams of Fig. 1, and with conditions of the two final-state photons being within the pseudorapidity range $|\eta| < 0.9$, and having an energy $E_{\mathrm{phot}} > 200$ MeV.

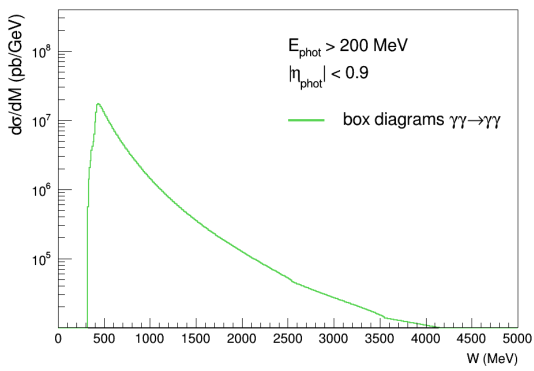

Fig. 2. Differential cross section $\mathrm{d}\sigma/\mathrm{d}M$ for photon scattering in PbPb collisions.

4. Resonance signal from η, η' decays

The cross section for photoproduction of η, η' is taken according to [7]

$$\sigma_{\gamma\gamma\to R} = 8\pi(2J+1)\frac{\Gamma_{\gamma\gamma}\Gamma_{\mathrm{tot}}}{\left(W^2 - M_R^2\right)^2 + M_R^2\Gamma_{\mathrm{tot}}^2} \, . \tag{4}$$

The cross section for photoproduction of η, η' in PbPb collisions is calculated according to the convolution defined in Eq. (3).

The η, η' cross section in PbPb collisions at $\sqrt{s} = 5.02$ TeV multiplied by the branching ratio $\eta, \eta' \to \gamma\gamma$ is shown in Fig. 3. The values shown are derived with conditions of the two decay photons being within the pseudorapidity range $|\eta| < 0.9$, and having an energy $E_{\mathrm{phot}} > 200$ MeV. The finite width of these two resonances results from the detector resolution of the photon measurements which is taken here to be $\sigma_{E_{\mathrm{phot}}}/E = 0.02$.

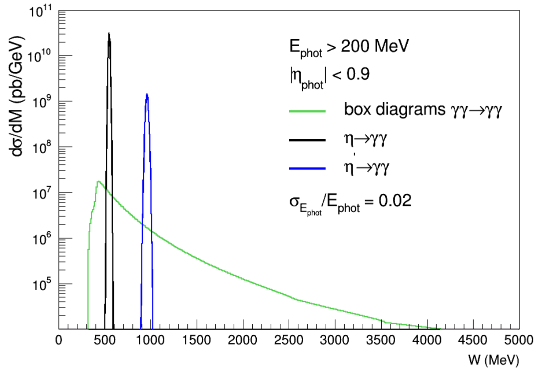

Fig. 3. Cross section for photoproduction of η, η'.

5. Photoproduction of $\pi^0\pi^0$ pairs

The main background to the signal of two photons in the final-state results from $\pi^0\pi^0$ production with two of the four decay photons escaping detection. The two measured photons from this $\pi^0\pi^0$ decay cannot be distinguished from the signal of photon–photon scattering.

The contribution of resonance decays to the $\pi^0\pi^0$ final state is shown in Fig. 4 on the left. Here, the resonances $f_0(600)$, $f_0(980)$, $f_0(1500)$, $f_0(1710)$, $f_2(1270)$, $f_2'(1525)$, $f_2(1565)$, $f_2(1950)$ and $f_4(2050)$ are considered [8]. The cross section $\gamma\gamma \to \pi^+\pi^-$ is much larger than for $\gamma\gamma \to \pi^0\pi^0$, hence even a small coupling between the charged and neutral pion channel might have an influence on the $\gamma\gamma \to \pi^0\pi^0$ cross section. Examples of processes leading to such channel couplings are shown in Fig. 4 in the middle and on the right.

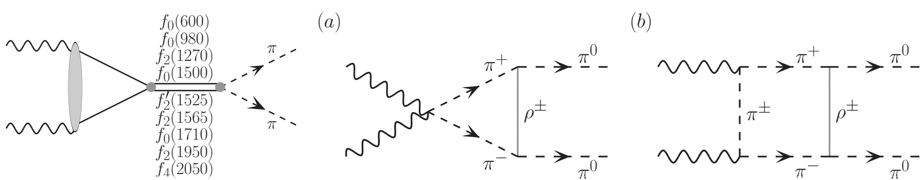

Fig. 4. Mechanisms of $\pi^0\pi^0$ photoproduction (figure taken from [8]).

6. Background from $\pi^0\pi^0$ decays

The $\pi^0\pi^0$ cross section in PbPb collisions is calculated by convoluting the elementary $\pi^0\pi^0$ cross section with the photon flux according to Eq. (2). The background from $\pi^0\pi^0$ decays is shown in Fig. 5 by the thick solid grey/red line. This background cross section is derived by the conditions that exactly one decay photon from each of the two π^0s is within the pseudorapidity range $|\eta| < 0.9$, and that these photons have an energy $E_{\rm phot} > 200$ MeV.

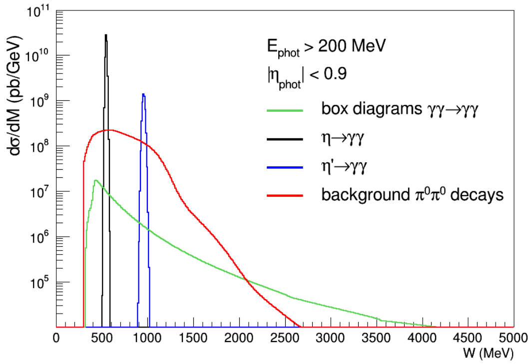

Fig. 5. (Colour on-line) Signal and background from $\pi^0\pi^0$ decays.

6.1. Background suppression by asymmetry cuts

The two photons of the signal are of equal transverse momentum and are back-to-back in azimuth. These correlations are smeared out due to finite resolution in the measurement of photon energy and azimuthal angle. The two photons from $\pi^0\pi^0$ decay do not show these correlations. A scalar ($A_{\rm S}$) and vector ($A_{\rm V}$) asymmetry can be defined for background suppression

$$A_{\rm S} = \left|\frac{|\vec{p}_{\rm T}(1)| - |\vec{p}_{\rm T}(2)|}{|\vec{p}_{\rm T}(1)| + |\vec{p}_{\rm T}(2)|}\right| , \qquad A_{\rm V} = \frac{|\vec{p}_{\rm T}(1) - \vec{p}_{\rm T}(2)|}{|\vec{p}_{\rm T}(1) + \vec{p}_{\rm T}(2)|} . \tag{5}$$

The background reduction for condition $A_{\rm S} < 0.1$ and $A_{\rm S} < 0.02$ is shown in Fig. 6 by the blue dash-dotted and red dashed line, respectively. The condition $A_{\rm S} < 0.02$ reduces the background by about a factor ~ 10 while keeping 98% of the signal.

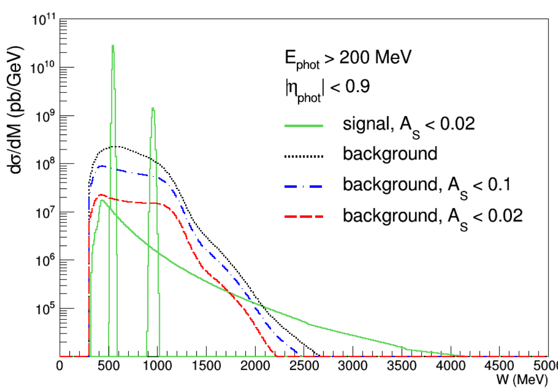

Fig. 6. (Colour on-line) Background suppression by asymmetry cut $A_{\rm S}$.

6.2. Background correction by sideband subtraction

The background remaining after the cut $A_{\mathrm{S}} < 0.02$ can be subtracted by sideband correction. The signal band is given by $0.0 < A_{\mathrm{S}} < 0.02$, with sideband 1 and 2 defined by $0.02 < A_{\mathrm{S}} < 0.04$ and $0.04 < A_{\mathrm{S}} < 0.06$, respectively. An estimator for the background in the signal region can be defined by linear extrapolation of the sidebands 1 and 2 into the signal region.

The background remaining after sideband correction is shown in Fig. 7 by the black/red line. The sideband correction could be further improved by defining more than two sidebands, and by a non-linear extrapolation of the background into the signal region.

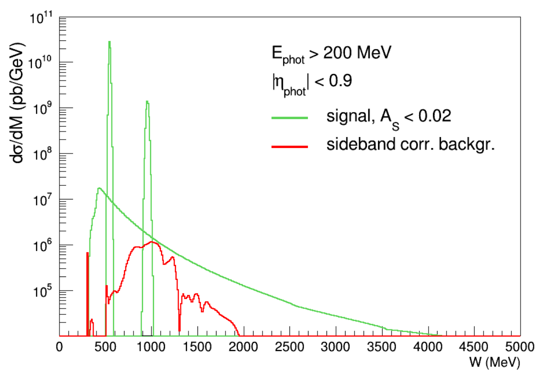

Fig. 7. (Colour on-line) Sideband corrected background.

This work is supported by the German Federal Ministry of Education and Research under promotional reference 05P15VHCA1.

REFERENCES

[1] M. Born, *Nature* **132**, 282 (1933).
[2] W. Heisenberg, H. Euler, *Z. Phys.* **98**, 714 (1936).
[3] ATLAS Collaboration, *Nature Phys.* **13**, 852 (2017).
[4] CMS Collaboration, `arXiv:1810.04602 [hep-ex]`.
[5] M. Kłusek-Gawenda *et al.*, *Phys. Rev. C* **93**, 044907 (2016).
[6] G. Baur *et al.*, *Phys. Rep.* **364**, 359 (2002).
[7] V.M. Budnev, I.F. Ginzburg, G.V. Meledin, V.G. Serbo, *Phys. Rep.* **15**, 181 (1975).
[8] M. Kłusek-Gawenda, A. Szczurek, *Phys. Rev. C* **87**, 054908 (2013).